GEOLOGICA CARPATHICA, JUNE 2012, 63, 3, 191–200 doi: 10.2478/v10096-012-0016-4

Permian volcanics in the Northern Gemericum and Bôrka Nappe system: U-Pb zircon dating and the implications for geodynamic evolution (Western Carpathians, Slovakia)

ANNA VOZÁROVÁ[1], MILOŠ ŠMELKO[1], ILYA PADERIN[2] and ALEXANDER LARIONOV[2]

[1]Comenius University in Bratislava, Faculty of Natural Sciences, Department of Mineralogy and Petrology, Mlynská dolina, Pav. G, 842 15 Bratislava, Slovak Republic; vozarova@fns.uniba.sk
[2]All-Russian Geological Research Institute (VSEGEI), Sredny prospect 74, 199 106 St.- Petersburg, Russia

(Manuscript received August 24, 2011; accepted in revised form September 30, 2011)

Abstract: U-Pb dating (SHRIMP) of magmatic zircon ages from the Northern Gemericum Permian volcanics (Petrová Hora Formation) yielded the Concordia age of 272.4 ± 7.3 Ma for basaltic andesite, as well as the Concordia age of 275.2 ± 4 Ma for rhyodacites. Both zircon ages correspond to the Cisuralian Epoch in the time span of the Kungurian Stage. Acquired $^{206}Pb/^{238}U$ zircon age data support the nearly contemporaneous origin of the acid and basic volcanogenic members in the Northern Gemericum Permian strata. The bimodal volcanic suite proves the transtension/extension tectonic regime in the North Gemeric sedimentary basin during the Late Cisuralian. The magmatic zircon ages of rhyodacites, occurring in the lower thrust sheet of the Bôrka Nappe (Jasov Formation), gave a younger Concordia age of 266 ± 1.8 Ma proving the Guadalupian Epoch, in the time span of the Wordian/Capitanian. In comparison to the Northern Gemericum realm, this age refers to the relatively younger stage of rift-related extensional movements. In the wide Alpine-Dinarides realm the Middle Permian (Guadalupian) movements are related to the beginning of the Alpine sedimentary cycle. Thus, the Middle Permian rifting expresses the beginning of the formation of the future Meliata oceanic trough.

Key words: Permian volcanism, Western Carpathians, geodynamic evolution, zircon ages.

Introduction

Permian coarse-grained sediments of the Northern Gemericum Unit unconformably overlap erosive relics of the Pennsylvanian and Mississippian sedimentary sequences, as well as both pre-Carboniferous crystalline complexes, Klátov and Rakovec. As the deposits of the continental arid to semiarid climate, they lack any relevant faunal and floral age evidence. The only possibility to prove their stratigraphic position is radiometric dating of the accompanied synsedimentary volcanic/volcaniclastic members. The first U-Pb dating from the uranium-bearing horizon in the Novoveská Huta ore deposits gave 240 ± 30 Ma, and was interpreted as the age of stratiform mineralization (Arapov et al. 1984). The newest monazite ages in the rhyolite tuff from the same locality confirm the age of 278 ± 10 Ma (Rojkovič & Konečný 2005). The Permian sedimentary sequence includes several volcanogenic horizons, with acid and intermediate/basic members, thus in situ U-Pb SHRIMP zircon dating (Laboratory of VSEGEI, Sankt Petersburg) has been applied, with the main objective of proving the age of magmatism and to specify the stratigraphy of the associated deposits.

The separate tectonic unit termed the Bôrka Nappe, considered as a high-pressure part of the Meliaticum Unit, contains in its basal part the coarse-grained metasedimentary complex with synsedimentary rhyodacites. No fossils were found due to the strong metamorphic and structural reworking of this sequence. Its Permian age was presupposed based on lithofacial similarities with the lower part of the Southern Gemeric Permian sequence (the Rožňava Formation). Therefore, our investigation is focused on determination the age of rhyodacites and the confirmation of stratigraphic specification and position of the subdivided lithostratigraphic unit, compared to analogous sequences in the Western Carpathians.

In this study we follow the time-scale calibration of Gradstein et al. (2004) in order to compare geochronological data from volcanic rocks with fossil bearing, sedimentary units.

Geological setting

The Western Carpathians orogenic belt is divided into an Outer belt that is made up of neo-Alpine nappes (Outer Western Carpathians), and an Inner belt (Inner Western Carpathians), with the pre-Gosau nappe system overlain by the Late Cretaceous to Tertiary volcanic-sedimentary formations. The Inner Western Carpathians consists of principal thick-skinned crustal-scale superunits made up of the pre-Alpine crystalline basement and its Late Paleozoic/Mesozoic envelope and several cover and rootless nappe systems. The Northern Gemericum belongs to the pre-Gosau nappe system of the Inner Western Carpathians (Biely et al. 1996 and references therein). The innermost part of the Western Carpathians is characterized by the extreme Early Cretaceous shortening due to the paleo-Alpine nappe stacking. Besides the basic supracrustal units, formed by the Northern and Southern Gemericum basement and their dominant Late Paleozoic envelope, several rootless nappe systems are present. The lowermost is

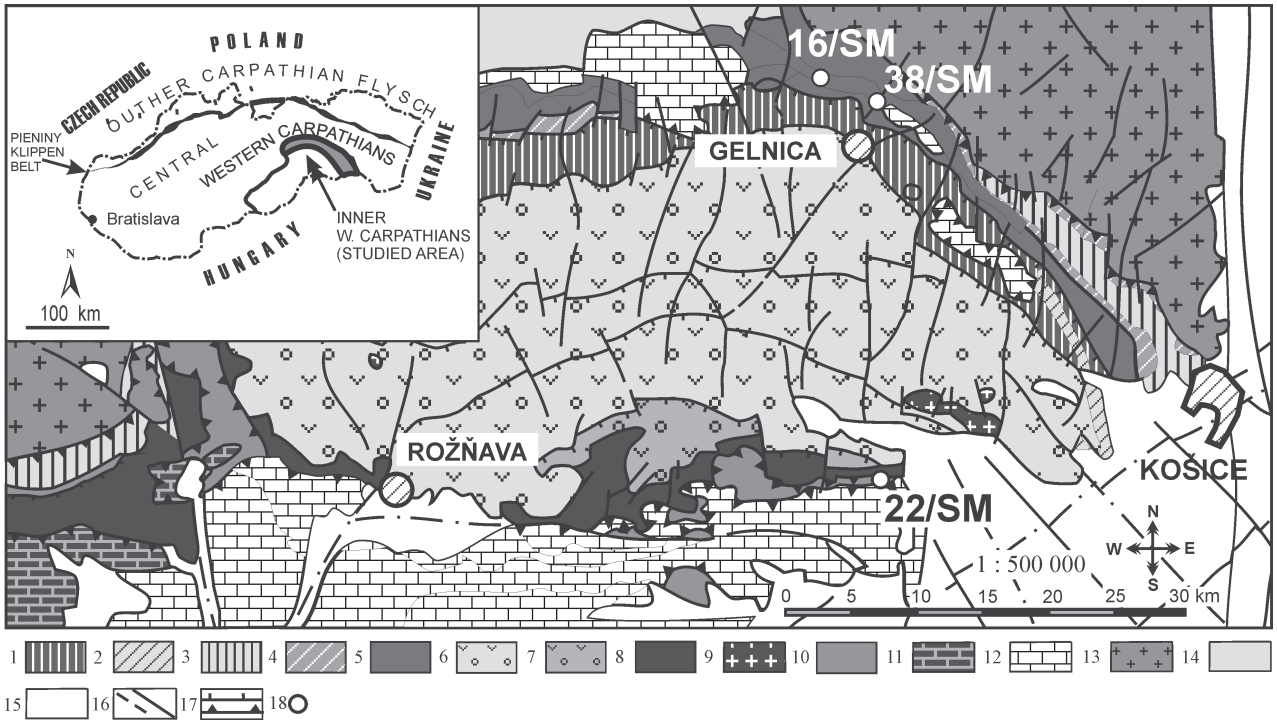

Fig. 1. Schematic geological map of the Inner Western Carpathians with indication of sample localities (modified after Bezák et al. 2004). Explanations: ***Northern Gemericum* (1–5)**: 1 — metapelites, metabasalts and their metavolcaniclastics of the Rakovec Complex; 2 — amphibolites and gneisses of the Klátov Complex; 3 — Mississippian formations; 4 — Pennsylvanian formations; 5 — Permian formations; ***Southern Gemericum* (6–9)**: 6 — turbidite metasediments and metavolcanites/metavolcaniclastics of the Gelnica Group, 7 — turbidite metasediments of the Štós Formation, 8 — Permian overstep sequence, 9 — Permian apical granites; **10** — *Meliaticum Unit* including the Bôrka Nappe sequence; **11** — *Turnaicum Unit* — Mesozoic and Late Paleozoic sequences; **12** — *Silicicum Unit* — Mesozoic sequences; **13** — *Veporicum* basement and its envelope sequence; **14** — Central Paleogene sediments; **15** — Neogene sediments; **16** — Main faults; **17** — Thrust fault, thrust plane; **18** — Selected localities for the magmatic zircon dating presented in this paper.

the Meliaticum Unit that was overthrusted by the Turnaicum and Silicicum thrust nappe system. The Bôrka Nappe, with relics of glaucophanites that immediately overthrusts the Gemericum, displays lithological and tectonic affinity to the Meliaticum Unit (Mello et al. 1998).

The Northern Gemericum: Bimodal, rhyolite-andesite/basalt volcanism is a characteristic member of the Northern Gemeric Permian sequences (Fig. 1); wide-spread within the Petrová Hora Formation (Fig. 2). Pulses of volcanic activity correspond to large regional sedimentary cycles triggered by an extensional regime. It is the most characteristic feature of the Petrová Hora Formation. Bimodal volcanism was dominated by rhyolite-dacite members, accompanied by subordinate andesites and basaltic andesites (Ivanov 1953; Rojkovič & Vozár 1972; Václav & Vozárová 1978). Sediments of the Petrova Hora Formation are characterized by the low degree of mineral and

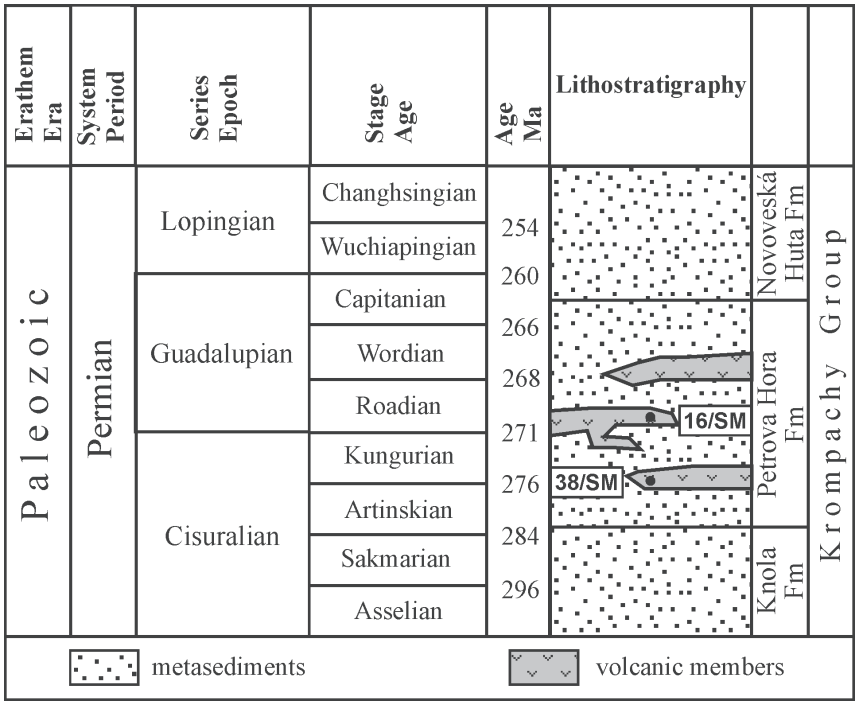

Fig. 2. North Gemeric Permian lithostratigraphic scheme with indication of magmatic zircon samples (modified after Vozárová 1996).

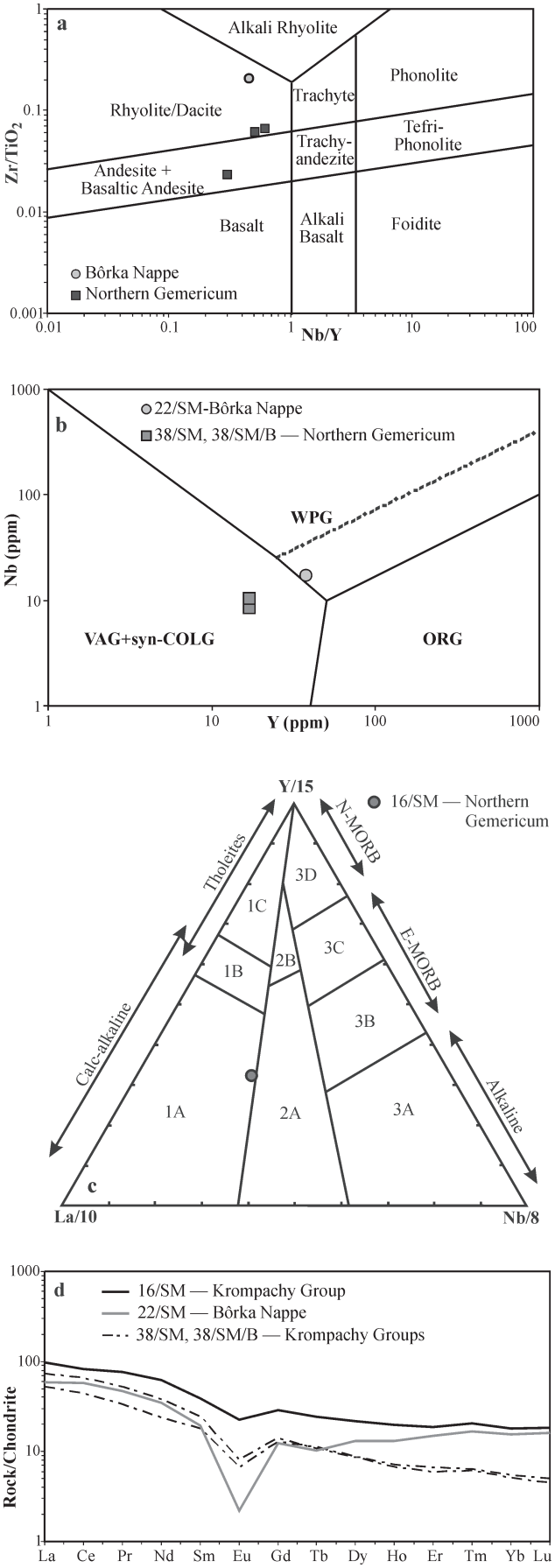

structural maturity. The compositional mixing of the syngenetic volcanic and extraformational non-volcanic detritus is very common. Among the most striking features are the fining-upward alluvial cycles, with channel lag, point-bar and flood-plain lithofacies, alternating with playa and ephemeral lake sub-environments at the topmost part of the large regional cycles.

Permian sequences of the Northern Gemericum are slightly deformed and recrystallized, under the metamorphic P-T conditions attaining P-T conditions from anchizone to the low-temperature part of greenschist facies (Šucha & Eberl 1992). The newly formed metamorphic mineral assemblage is represented by the fine-grained aggregate of quartz + illite + chlorite ± albite and/or microcline.

The Permian volcanites of the Northern Gemericum vary from peraluminous acid to the metaluminous intermediate/basic volcanic rock suites, with Shand's Index diagram in the range of values A/CNK = 0.92–3.48 and A/NK = 1.29–3.51. As the studied volcanites manifest strong secondary alteration, in conformity with variability of Shand's index, their classification was based on incompatible elements Zr/TiO_2 vs. Nb/Y (Winchester & Floyd 1977). They compile a continuous volcanic suite from rhyolites and dacites to andesite and basaltic andesite (Fig. 3a). Selected trace elements (Nb, Ta, Y, and Yb) suggest these acid volcanites were formed in a post-collisional tectonic setting (Fig. 3b), but with distinct affinity to the syn-collisional magmatites in chemical composition. Basaltic andesite, based on Y : La : Nb ratio point to a continental calc-alkaline basalt suite (Fig. 3c). Chondrite-normalized REE abundances (Fig. 3d) in the acid volcanites are enriched on light REE and have relatively fractionated heavy REE with $(La/Yb)_n$ between 10 and 12 and $(La/Sm)_n$ between 2.1 and 3.2. Compared to this, chondrite-normalized REE abundances in the basaltic andesite have relatively unfractionated heavy REE with $(LA/Yb)_n = 5$ and $(La/Sm)_n = 1.6$ (Fig. 3d).

The Bôrka Nappe: The Bôrka Nappe is composed of a changeable, incoherent and tectonically intensively segmented package of the Alpine medium- to high-pressure metamorphosed volcano-sedimentary complex of Permian-Jurassic age (Fig. 4). It comprises an accretionary prism rock complex formed by the Late Triassic-Jurassic subduction of the oceanic crust and adjacent continental margin of the Meliata Ocean (Mello et al. 1998). The tectonic individualization of this ac-

Fig. 3. Northern Gemeric and Bôrka Nappe dated volcanite characteristics based on their chemical composition. **a** — Zr/TiO_2 (wt. %) vs. Nb/Y (ppm) classification diagram after Winchester & Floyd (1977). **b** — Variations Nb (ppm) vs. Y (ppm) in the acid volcanites with indication of tectonic setting after Pearce et al. (1984); Abbreviations: **WPG** — within-plate granite, **ORG** — orogenic granite, **VAG + syn-COLG** — volcanic arc and syn-collisional granite. **c** — Position of basaltic andesite (sample no. 16/SM) in the Y/15 : La/10 : Nb/8 discrimination diagram after (Cabanis & Leccole 1989); Abbreviations: **1A** — calc-alkaline basalts, **1B** — calc-alkaline basalts and island-arc tholeiites, **1C** — island arc tholeiites, **2A** — continental basalts, **2B** — back-arc basin basalts, **3A** — alkali basalts of within-continental rift, **3B** — enriched E-MORB, **3C** — slightly enriched E-MORB, **3D** — N-MORB. **d** — Chondrite normalized REE patterns. Normalizing values are after Taylor & McLennan (1985).

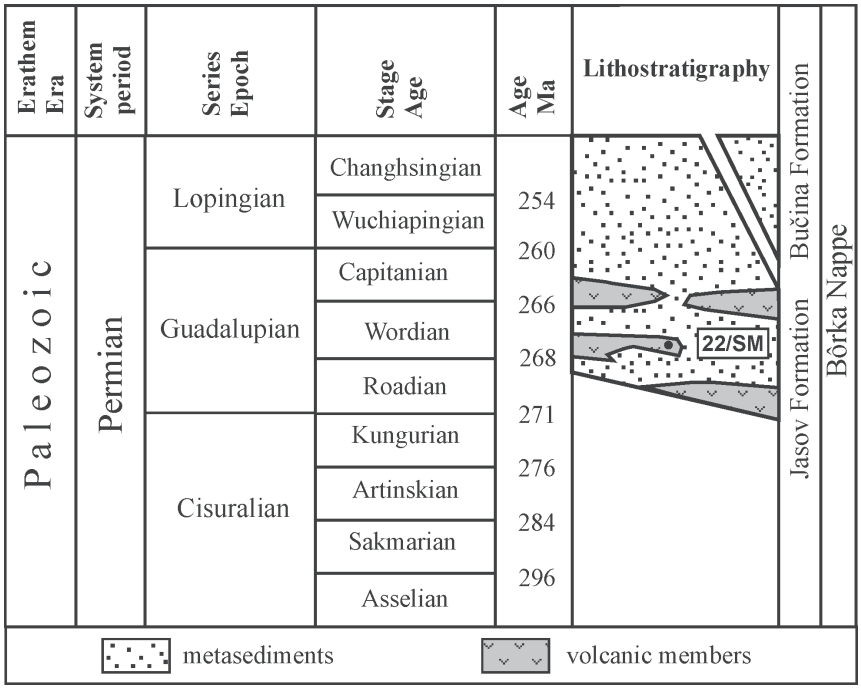

Fig. 4. Bôrka Nappe lithostratigraphic scheme with indication of magmatic zircon samples (modified after Mello et al. 1997, 1998).

cretionary prism and its transport into the present structural position was attained during the nappe stacking stage in the Early Cretaceous. On the basis of the lithology and mutual relationships of the individual lithological complexes, the Bôrka Nappe is subdivided into several lithostratigraphic units, includig the Jasov Formation of the basal thrust sheet (Mello et al. 1997, 1998).

The *Jasov Formation* consists of a monotonous sequence of siliciclastic metasediments, mostly metapsamites interlayered with metaconglomerates in its lower part and with metasiltstones and metapelites in its upper part. The metarhyolites and their volcaniclastics comprise smaller bodies and lense-shaped layers in the lower part of the Jasov Formation (Fig. 4). A Permian age was presupposed on the basis of lithological similarities with the Southern Gemericum Permian sediments of the Gočaltovo Group (Mello et al. 1998). The Jasov Formation, inspite of the lithological similarities, significantly differs from the Southern Gemericum Permian by the character of metamorphic and structural alteration. The metamorphic mineral associations (Cld + Chl + Ab + Phn ± Pg) and $b_{331,060}$ spacing of potash white mica, proved temperatures around 350–400 °C at middle-high pressure regime during climax of the Alpine metamorphism (Mazzoli et al. 1992).

The whole rock chemical analyses of volcanites indicate rhyolite-dacite composition. This is also confirmed by trace elements — Nb/Y vs. Zr/TiO_2 (Winchester & Floyd 1997) classification, based on the ratios of Nb/Y vs. Zr/TiO_2 (Fig. 3a). According to Shand's Index, with values of A/CNK = 1.59–2.64 and A/NK = 1.61–2.77 the Jasov Formation acid volcanites correspond to the peraluminous suite. The Nb:Y ratio indicates a within-plate origin (Fig. 3b). Chondrite-normalized REE pattern in the Bôrka Nappe rhyodacite is enriched in light REE and have relatively unfractionated heavy REE (Fig. 3d), with $(La/Yb)_n$ ratio of 3.2 and $(La/Sm)_n$ ratio of 2.7. The distinct negative Eu anomaly is indicative of extensive fractional crystallization involving plagioclase. According to the selected trace elements, mainly Nb–Y–Ce, the rocks fit into the A_2-type post-orogenic magmatic suite (in the sense of Eby et al. 1992), with ratios Y/Nb >1.2. The increased content of Rb (70–262 ppm), Zr (254–600 ppm), Y (28–72 ppm) and rare earth elements excluding Eu (0.66–1.24 ppm) along with low content of Sr (6–21 ppm) and V (8–74 ppm) is their characteristic feature.

Analytical method

Zircons were separated from rocks by standard grinding, heavy liquid and magnetic separation analytical procedures. The internal zoning structures and shapes of the half-sectioned zircon crystals mounted in epoxy resin puck with chips of the TEMORA (Middledale Gabbroic Diorite, New South Wales, Australia Black et al. 2003) and 91500 (Geostandard zircon, Wiedenbeck et al. 1995) reference zircons, were imaged by optical microscopy, BSE and CL, in order to guide analytical spots positioning. *In situ* U-Pb analyses were performed on a SHRIMP-II in the Center of Isotopic Research (CIR) at VSEGEI in St.-Petersburg, Russia.

Each analysis consisted of 5 scans through the 196–254 AMU mass range; primary beam diameter was about 25 μm, with intensity of ca. 6 nA. The data were reduced in a manner similar to that described by Williams (1998, and references therein), using the SQUID Excel Macro of Ludwig (2000). The Pb/U ratios were normalized relative to a value of 0.0668 for the $^{206}Pb/^{238}U$ ratio of the TEMORA reference zircons, equivalent to an age of 416.75 Ma (Black et al. 2003); common lead was corrected using measured $^{204}Pb/^{206}Pb$ (Stacey & Kramers 1975). Age calculations and plotting was done with ISOPLOT/EX (Ludwig 1999). Uncertainties given for individual analyses (ratios and ages) are at the one σ level; however the uncertainties in calculated concordia ages are reported at two σ levels.

All dated samples were analysed for major and trace elements content including REE. Their chemical composition was determined by ICP/ICP-MS in ACME Laboratories Ltd., Vancouver, Canada.

Results

***Northern Gemericum — Petrova Hora Formation*:** Two samples from the Petrova Hora Formation were investigated:

i) Sample no. ***38/SM*** from the vicinity of Jaklovce village (N 48°52′160″, E 20°58′723″, 356 m above see level) have the rhyodacite composition. The fine-grained microporphyric texture is formed by the small phenocrysts of β-quartz, perthitic K-feldspars and rare Na-Ca feldspars. Mafic minerals are represented by scarce, strongly altered biotite. Besides the small grains of quartz the blastofelzitic matrix contains relic thin crystallites of feldspars. Zircon, monazite, xenotime, apatite, rutile and Fe-Ti oxides are present as the accessory minerals. Major and trace element analyses are presented in Table 1.

The U-Pb dating has been carried out on ten zircon grains. Seven of them have euhedral shapes, and are 40–70×250–350 μm in size. Th/U ratios range from 0.10 to 0.63 (Table 2). These seven results are similar in $^{206}Pb/^{238}U$ ratios and are considered to be a single population. The Concordia age of 275.2 ± 4 Ma (Fig. 5) is interpreted as the igneous crystallization age of the rhyodacite.

The other four analyses, three from the single grains and one from the inherited core within the volcanic zircon crystal (spot 6.1 in the Table 2), yielded Neoproterozoic ages (Ediacaran) spanning from 602 to 637 Ma with Th/U ratios ranging from 0.16 to 0.94. Their subhedral or rounded morphologies and significantly older apparent ages suggest their xenocrystic nature: possibly they were entrained from sedimentary wall-rock or the volcanics protolith.

ii) The basaltic andesite sample no. ***16/SM*** has been collected S of Krompachy town (N 48°55´074″, E 20°53´18″, 445 m above see level). The sample is dark rock, and has aphanitic and fine-grained texture, with rare preserved phenocrysts (max. 3 %). Plagioclase phenocrysts are the most abundant phase. Fe-Ti oxides are present ubiquitously both as microphenocrysts and, in higher amounts, as a groundmass phase. The whole rock is strongly altered. The main secondary minerals are chlorite, calcite and sericite. The bulk chemical composition as well as the trace elements composition including REE concentration is given in Table 1.

The only two zircons from the analysed set gave Permian ages 270.7 ± 5.3 Ma and 273.6 ± 5.3 Ma. Both zircons show features typical of magmatic zircon from basic rocks: high Th/U ratios (1.2–2.6), with relatively high contents of U (829 and 1257 ppm) and Th (1020 and 3238 ppm) (Table 2) and poorly pronounced growth zoning. These youngest $^{206}Pb/^{238}U$ ages are interpreted as the best estimate of the basaltic andesite extrusion time.

Seven of eleven analysed zircons from basaltic andesite 16/SM cluster between 526 and 476 (Fig. 6) with weighted average $^{206}Pb/^{238}U$ of 504 ± 16 Ma. Elevated MSWD = 3.1 along with widely variable Th/U = 0.05–1.18 assume this is heterogeneous group. Selection of zircons with Th/U < 0.2 (see Table 2) gives weighted average of 497 ± 18 (MSWD = 2.4). Of four ca. 520–660 Ma old zircons three have Th/U > 1 typical of zircon from mafic or alkalic rocks. This feature is shared with the first two zircon grains (although their CL structure is different) with pooled Concordia Permian age of 272.4 ± 7.3 Ma (Fig. 6). All but the first two zircons display fine to coarse oscillatory zoning patterns, with growth zones locally interrupted by dissolution surfaces. These structures indicate zircon's magmatic origin, which is supported by the Th/U ratios (0.11–1.18). The two grains, with very low Th/U (0.05–0.08) may either be interpreted as metamorphic or postdating the Th-absorbing mineral phase in their parental rock; the latter might find succour in their CL-structure quite resembling magmatic. The Neoproterozoic ages were indicated within the two other magmatic zircon grains, with ages of 59311 Ma and 659 ± 12 Ma (Table 2).

All the Lower Paleozoic/Neoproterozoic zircon grains are interpreted as material recycled and reworked from the basement rocks possibly assuming prominence of ca. 500 Ma old rocks in the volcanites source.

Table 1: Northern Gemericum and Bôrka Nappe Permian volcanites rock chemical analyses.

Locality	Meliaticum	Northern Gemericum		
	Bôrka Nappe	Krompachy Group	Krompachy Group	Krompachy Group
Sample	22/SM	16/SM	38/SM	38/SM-B
	wt. (%)	wt. (%)	wt. (%)	wt. (%)
SiO_2	78.25	55.94	82.50	80.95
Al_2O_3	11.57	16.07	8.75	11.02
Fe_2O_3	2.72	9.02	2.25	2.22
MgO	0.40	1.85	1.71	0.30
CaO	0.04	3.58	0.04	0.07
Na_2O	2.57	4.91	0.06	0.18
K_2O	2.74	1.75	2.52	3.22
TiO_2	0.13	1.19	0.12	0.12
P_2O_5	0.03	0.60	0.05	0.07
MnO	0.02	0.09	0.01	0.03
Cr_2O_3	0.01	0.00	0.01	0.01
Ni	29.00	20.00	20.00	20.00
Sc	4.00	15.00	3.00	4.00
LOI	1.50	5.00	1.90	1.70
Total	99.92	100.03	99.87	99.90
	ppm	ppm	ppm	ppm
Hf	8.20	7.60	2.50	3.10
Nb	17.10	14.10	8.60	10.40
Rb	69.80	59.80	91.30	150.40
Sn	5.00	3.00	3.00	5.00
Sr	14.40	88.10	21.80	38.00
Ta	1.30	0.90	0.60	0.90
Th	19.60	9.70	12.20	9.70
U	4.50	2.40	0.90	2.40
V	24.00	57.00	11.00	17.00
W	3.90	0.90	1.30	0.90
Zr	270.70	279.00	73.50	79.80
Y	37.60	46.40	16.80	17.00
La	58.10	35.80	19.40	27.00
Ce	122.90	79.50	42.20	63.10
Pr	15.32	10.55	4.60	7.15
Nd	61.00	44.00	16.90	26.90
Sm	11.35	9.00	4.18	5.65
Eu	0.73	1.98	0.58	0.70
Gd	9.10	8.87	3.90	4.30
Tb	1.16	1.42	0.65	0.63
Dy	7.75	8.20	3.34	3.31
Ho	1.52	1.67	0.61	0.58
Er	4.19	4.64	1.67	1.48
Tm	0.67	0.73	0.23	0.22
Yb	4.21	4.45	1.37	1.28
Lu	0.62	0.70	0.19	0.17
La_N/Sm_N	3.22	2.50	2.92	3.01
La_N/Yb_N	9.33	5.44	9.57	14.25
Eu/Eu*	0.22	0.68	0.44	0.43

Table 2: Northern Gemericum and Bôrka Nappe Permian volcanites ion microprobe zircon data. Errors are 1-sigma; Pb_c and Pb^* indicate the common and radiogenic portion, respectively. (1) Common Pb corrected using measured ^{204}Pb.

Spot	% $^{206}Pb_c$	ppm U	ppm Th	ppm $^{206}Pb^*$	$\frac{^{232}Th}{^{238}U}$	(1) $\frac{^{206}Pb}{^{238}U}$ Age		(1) $\frac{^{207}Pb}{^{206}Pb}$ Age		% Dis-cor-dant	(1) $\frac{^{238}U}{^{206}Pb^*}$	±%	(1) $\frac{^{207}Pb^*}{^{206}Pb^*}$	±%	(1) $\frac{^{207}Pb^*}{^{235}U}$	±%	(1) $\frac{^{206}Pb^*}{^{238}U}$	±%	err corr
38/SM																			
4.1	0.00	392	190	14.1	0.50	264	± 5.2	299	±41	13	23.91	2	0.0523	1.8	0.3016	2.7	0.0418	2	0.75
5.1	0.21	327	201	12	0.63	270	± 6.3	276	±57	2	23.4	2.4	0.0518	2.5	0.305	3.5	0.0427	2.4	0.69
1.1	0.01	2711	267	101	0.10	273	± 5.2	269	±16	–2	23.13	2	0.0516	0.68	0.3078	2.1	0.0432	2	0.94
7.1	0.03	4040	832	153	0.21	278	± 5.3	280	±15	1	22.66	2	0.0519	0.67	0.3157	2.1	0.0441	2	0.95
6.2	0.13	2290	526	87.3	0.24	280	± 5.4	254	±29	–9	22.57	2	0.0513	1.3	0.3134	2.3	0.0443	2	0.84
2.1	0.05	1979	151	75.6	0.08	280	± 5.4	270	±23	–4	22.5	2	0.0516	1	0.3165	2.2	0.0445	2	0.89
3.1	0.15	366	202	14.1	0.57	283	± 5.7	254	±51	–10	22.3	2.1	0.0513	2.2	0.3171	3	0.0448	2.1	0.68
6.1	0.03	533	83	44.8	0.16	602	± 11	550	±24	–9	10.22	2	0.0586	1.1	0.79	2.3	0.0978	2	0.87
8.1	0.12	301	264	25.6	0.90	609	± 12	551	±38	–10	10.1	2	0.0586	1.7	0.799	2.7	0.099	2	0.76
10.1	0.15	146	133	13	0.94	633	± 12	582	±61	–8	9.69	2.1	0.0594	2.8	0.846	3.5	0.1032	2.1	0.59
9.1	0.29	569	134	50.9	0.24	637	± 12	532	±35	–17	9.63	2	0.0581	1.6	0.831	2.6	0.1039	2	0.77
16/SM																			
5.1	0.00	829	1020	30.6	1.27	271	± 5.3	271	±30	0	23.32	2	0.0517	1.3	0.3055	2.4	0.0429	2	0.83
6.1	0.00	1254	3238	46.7	2.67	274	± 5.3	283	±23	3	23.07	2	0.0519	10	0.3104	2.2	0.0434	2	0.89
7.1	0.09	484	23	31.9	0.05	476	± 9.1	484	±30	2	13.04	2	0.0568	1.3	0.601	2.4	0.0767	2	0.83
8.1	0.10	255	44	17.4	0.18	492	± 9.6	504	±42	2	12.6	2	0.0573	1.9	0.627	2.8	0.0794	2	0.73
4.1	0.00	432	34	29.9	0.08	499	± 9.7	486	±29	–3	12.42	2	0.0569	1.3	0.631	2.4	0.0805	2	0.84
9.1	0.00	297	45	20.8	0.16	506	± 9.8	527	±32	4	12.26	2	0.0579	1.4	0.652	2.5	0.0816	2	0.81
10.1	0.08	332	36	23.7	0.11	515	± 9.9	544	±79	6	12.03	2	0.0584	3.6	0.669	4.1	0.0831	2	0.49
1.1	0.17	365	354	26.2	1.00	518	± 10	520	±36	0	11.96	2	0.0578	1.7	0.666	2.6	0.0836	2	0.77
2.1	0.21	1094	1245	80.1	1.18	526	± 10	517	±35	–2	11.76	2.1	0.0577	1.6	0.676	2.6	0.0850	2.1	0.79
3.1	0.02	890	866	73.9	1.01	595	± 11	532	±19	–11	10.35	2	0.0581	0.86	0.773	2.2	0.0966	2	0.92
11.1	0.15	1038	517	96.2	0.51	659	± 12	565	±20	–14	9.28	2	0.0589	0.94	0.875	2.2	0.1077	2	0.90

Errors are 1-sigma; Pb_c and Pb^* indicate the common and radiogenic portions. respectively.
Error in TEMORA Standard calibration was 0.59 %. (1) Common Pb corrected using measured ^{204}Pb.

Spot	% $^{206}Pb_c$	ppm U	ppm Th	ppm $^{206}Pb^*$	$\frac{^{232}Th}{^{238}U}$	(1) $\frac{^{206}Pb}{^{238}U}$ Age		(1) $\frac{^{207}Pb}{^{206}Pb}$ Age		% Dis-cor-dant	(1) $\frac{^{238}U}{^{206}Pb^*}$	±%	(1) $\frac{^{207}Pb^*}{^{206}Pb^*}$	±%	(1) $\frac{^{207}Pb^*}{^{235}U}$	±%	(1) $\frac{^{206}Pb^*}{^{238}U}$	±%	err corr
22/SM																			
9.1	--	419	308	15.1	0.76	264	±3	270	±111	+2	23.9	1.1	0.0517	4.9	0.30	5.0	0.042	1.1	0.2
1.1	0.50	449	197	16.1	0.45	264	±3	133	±85	–101	23.9	1.1	0.0487	3.6	0.28	3.8	0.042	1.1	0.3
7.1	0.24	865	739	31.1	0.88	264	±3	239	±41	–11	23.9	1.0	0.0510	1.8	0.29	2.0	0.042	1.0	0.5
4.1	--	970	919	34.9	0.98	265	±3	293	±29	+10	23.9	1.0	0.0522	1.3	0.30	1.6	0.042	1.0	0.6
2.1	0.43	1488	1978	53.6	1.37	265	±3	312	±41	+16	23.8	1.2	0.0526	1.8	0.30	2.2	0.042	1.2	0.6
8.1	0.49	503	215	18.2	0.44	265	±3	273	±67	+3	23.8	1.1	0.0517	2.9	0.30	3.1	0.042	1.1	0.3
3.1	0.13	587	273	21.2	0.48	266	±4	300	±47	+12	23.8	1.7	0.0523	2.0	0.30	2.7	0.042	1.7	0.6
5.1	0.27	557	264	20.2	0.49	266	±3	304	±50	+13	23.7	1.0	0.0524	2.2	0.30	2.4	0.042	1.0	0.4
6.1	0.12	652	413	23.8	0.65	269	±3	303	±38	+12	23.5	1.0	0.0524	1.7	0.31	1.9	0.043	1.0	0.5
10.1	0.30	647	336	23.8	0.54	270	±3	301	±81	+10	23.3	1.0	0.0523	3.6	0.31	3.7	0.043	1.0	0.3

Errors are 1-sigma; Pb_c and Pb^* indicate the common and radiogenic portions. respectively.
Error in TEMORA Standard calibration was 0.28 %. (1) Common Pb corrected using measured ^{204}Pb.

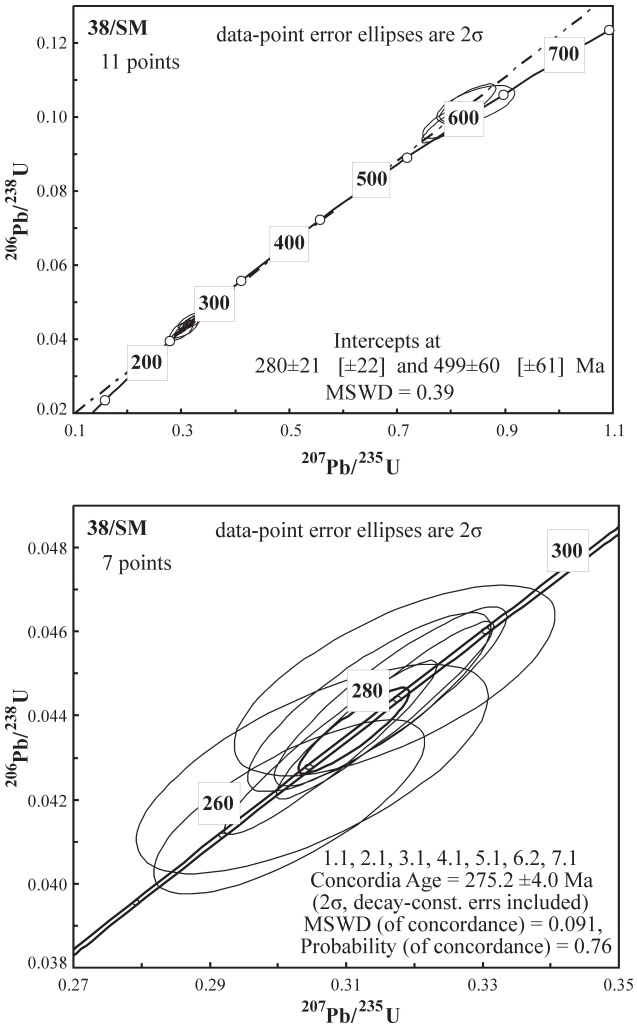

Fig. 5. Concordia diagrams of magmatic zircon ages from the Northern Gemericum rhyodacite (sample no. 38/SM).

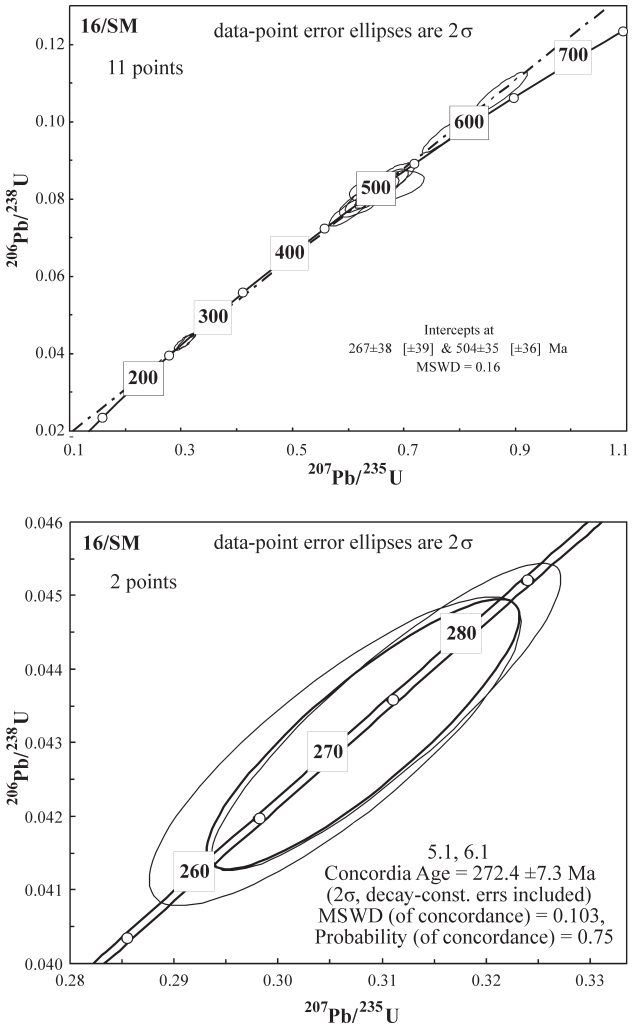

Fig. 6. Concordia diagrams of zircon age data from the Northern Gemeric basaltic andesite (sample no. 16/SM).

Bôrka Nappe — Jasov Formation*:** $^{206}Pb/^{238}U$ zircon ages were obtained from the metarhyodacite sample ***22/SM, collected in the abandoned quarry, situated west of Jasov village (N 48°40´626″, E 20°56´745″, 281 m above see level).

The Jasov Formation metavolcanites and metavolcaniclastics have dominant blastofelsitic and blastovitroclastic texture. Related metavolcanics contain a few deformed phenocrysts of quartz and abundant recrystallized volcanic glass in the groundmass. The newly formed metamorphic mineral assemblage is represented by the fine-grained aggregate of quartz + muscovite + phengite ± chlorite ± albite. Zircon, monazite, xenotime, apatite, and Fe-Ti oxides are present as accessory minerals. The representative chemical composition of sample 22/SM is given in Table 1.

In the zircons analysed the Th/U ranges 0.44–1.37 are typical for that from igneous rocks. The zircon crystals have euhedral shapes, characterized by the aspect ratios of ca. 1 : 2. Ten zircon analyses from the sample 22/SM form a very coherent cluster with $^{206}Pb/^{238}U$ 266 ± 1.8 Ma Concordia age (Fig. 7). This average $^{206}Pb/^{238}U$ age is interpreted as the magmatic crystallization age of the Jasov Formation metarhyodacite.

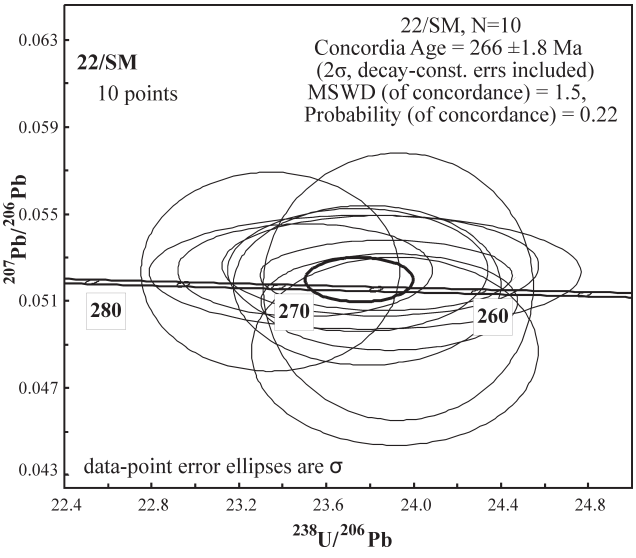

Fig. 7. Concordia diagram of zircon age data from the Bôrka Nappe rhyodacite (sample no. 22/SM).

Discussion

During the post-Variscan period an intense crustal re-equilibration and reorganization took place under alternating transtensional and transpressional tectonic regime. Following the main phases of Variscan compression, thermal relaxation of the crust occurred in Early Permian times, creating the rifts and grabens that allowed accumulation of the first phase of continental sediments (Ziegler 1990).

U-Pb (SHRIMP) magmatic zircon ages obtained from the Northern Gemericum Permian sequence proved 275 Ma (Artinskian/Kungurian) as the date of the main phase of rifting and volcanic activity. In contrast, the most voluminous and evolved magmatism occurred in the North German Basin (Benek et al. 1996) and is dated 297–302 Ma (Breitkreuz & Kennedy 1999). The Oslo Rift contains the most extensive and best preserved sequences of basaltic lavas associated also with this event (Naumann et al. 1992). The palynomorph assemblages from intravolcanic sediments from the Bolsano volcanic complex in the Southern Alps document its Artinskian-Kungurian age (Hartkopf-Fröder & Krainer 1990).

The obtained $^{206}Pb/^{238}U$ zircon age data from the Northern Gemericum Permian volcanites support the nearly contemporaneous origin of the acid and basic volcanogenic members. This bimodal volcanic suite proves the transtension/extension tectonic regime in the North Gemeric sedimentary basin during the upper Cisuralian, reflected by the bimodal magmatic activity. The crustal shortening within the Western Carpathian Variscan fold-and-thrust collisional belt terminated at the end of the Moscovian. Following the main phase of compression, the Cisuralian thermal relaxation of the newly formed crust, results in extension and associated block faulting, accompanied by corresponding magmatic activity (Saalian movements). A feeder rift system was formed for sediment transport from the Variscan belt as well as from the syngenetic volcanism to the irregularly subsiding basin.

The Carboniferous-Permian change from convergence to extension has been attributed by Stampfli et al. (2002) to collision of the Paleo-Tethys mid-ocean ridge with the trench bordering Laurussia. This tectonic setting produced pull-apart rift basins. The irregularity of the continental basin margin generated local zones of extension and compression. Although the North Gemeric volcanic rocks are bimodal, mafic types indicate affinity to a within-plate setting, derived from the subcontinental mantle during rifting. The analogous tectonic setting was supposed by Dostal et al. (2003) for the Hronicum sedimentary realm in the Central Western Carpathians.

The Neoproterozoic–Cambrian zircon ages from the North Gemeric volcanites indicate recycling processes and reworking from the older basement crust.

The $^{206}Pb/^{238}U$ zircon data from the Permian volcanites of the Bôrka Nappe yield essential younger ages of 266 ± 2 Ma. In comparison to the Northern Gemericum realm, this Guadalupian age (Wordian/Capitanian) refers to the relatively younger stage of rift-related extensional movement and derived volcanism. Equally, in the lithologically closest Southern Gemeric domain, the zircon population from the Rožňava Formation acid volcanites gave an older age of 275 Ma (Vozárová et al. 2009a). In the wide Alpine-Dinarides realm the Middle Permian (Guadalupian) movements are related to the beginning of the Alpine sedimentary cycle (Krainer 1993; Filipovič et al. 2003; Vozárová et al. 2009b). Generally, the thermal signature of the Permian rifting was a significant control of the subsequent Mesozoic and Cenozoic evolution of the European lithosphere. In the Meliaticum domain this continental Permian rifting was prolonged intensively in the Lopingian and Triassic and in their final stage led to the origin of the Meliata oceanic basin (Kozur 1991; Mello et al. 1998).

Conclusions

i) The $^{206}Pb/^{238}U$ zircon age data from the Northern Gemericum Permian volcanites confirm the Artinskian-Kungurian age (Cisuralian). The obtained data show that both, acid and basic members of the volcanogenic sequence are coeval. The Cisuralian thermal relaxation of the newly formed Variscan crust, resulted in extension and associated block faulting, accompanied by corresponding bimodal magmatic activity. A feeder rift system was formed for sediments transport from the Variscan belt as well as from the syngenetic volcanism to the irregularly subsiding basin.

ii) The $^{206}Pb/^{238}U$ zircon age data from the Bôrka Nappe (Meliaticum tectonic unit) acid volcanites indicate the Guadalupian volcanism. This information indicates the propagation of the continental rifting further into the foreland of the Variscan belt, closer to the northern margin of the Paleo-Tethys domain. Thus, the Middle Permian rifting expresses the beginning of the origin of the future Meliata oceanic trough.

Acknowledgment: The financial supports of the Slovak Research and Development Support Agency (Project ID: APVV-0438-06), as well as the Comenius University Bratislava Grant Agency (Project UK 527/2010) are gratefully acknowledged. We also thank Professor Fritz Ebner and dr. Pavol Siman for their useful comments and suggestions.

References

Arapov J.A., Bojcov V.J., Česnokov N.I., Djakonov A.V., Halbrštát J., Jakovjenko A.M., Kolek M., Komínek J., Kozyrev V.N., Kremčukov G.A., Lažanský M., Milovanov I.A., Nový V. & Sorf V. 1984: Czechoslovak uranium ore deposits. [Československá ložiska uranu.] *STNL*, Praha, 1–365 (in Czech).

Benek R., Kramer W., McCann T., Scheck M., Negendank J.F.W., Korich D., Huebscher H.-D. & Bayer U. 1996: Permo-Carboniferous magmatism of the Northeast German Basin. *Tectonophysics* 266, 379–404.

Biely A., Bezák V., Elečko M., Gross P., Kaličiak M., Konečný V., Lexa J., Mello J., Nemčok J., Potfaj M., Rakús M., Vass D., Vozár J. & Vozárová A. 1996: Explanation to Geological Map of Slovakia. *Ministry of the Environment of Slovak Republic, Geological Survey of Slovak Republic*, Bratislava, 1–76.

Black L.P., Kamo S.L., Allen C.M., Aleinikoff J.N., Davis D.W., Korsch R.J. & Foudoulis C. 2003: TEMORA 1: a new zircon standard for Phanerozoic U-Pb geochronology. *Chem. Geol.* 200, 155–170.

Breitkreuz C. & Kennedy A. 1999: Magmatic flare-up at the Carbon-

iferous-Permian boundary in the NE German Basin revealed by SHRIMP zircon ages. *Tectonophysics* 302, 307–326.

Cabanis B. & Leccole M. 1989: Le diagramme La/10-Y/15- Nb/8: un outil pour la discrimination des series volcaniques et la mise en evidence des processus de mélange et/ou de contamination crustale. *C.R. Acad. Sci. Paris*, *Ser. II* 309, 2023–2029.

Dostal J., Vozár J., Keppie J.D. & Hovorka D. 2003: Permian volcanism in the Central Western Carpathians (Slovakia): Basin-and-Range type rifting in the southern Laurussian margin. *Int. J. Earth Sci. (Geol. Rundsch.)* 92, 27–35. Doi: 0.1007/s00531-002-0307-6

Eby N.G. 1992: Chemical subdivision of the granitoids: Petrogenetic and tectonic implications. *Geology* 20, 641–644.

Filipović I., Jovanović D., Sudar M., Pelikán P., Kovács S., Less Gy. & Hips K. 2003: Comparison of the Variscan — Early Alpine evolution of the Jadar Block (NW Serbia) and "Bükkium" (NE Hungary) terranes; some paleogeographic implications. *Slovak Geol. Mag*. 9/1, 3–21.

Gradstein F.M., Ogg J.G., Smith A.G., Bleeker W. & Lourens L.J. 2004: A new Geological Time Scale with special reference to Precambrian and Neogene. *Episodes* 27, 2, 83–100.

Hartkopf-Fröder C. & Krainer K. 1990: Fluviatile und lakustrine Sedimente innerhalb der permischen Bozener Quartzporphyrabfolge (Südtirol/Italien): Ihre biostratigraphische und paläoekologische Bedeutung. *Sediment '90*, Bonn (Abstr.), *Geol. Inst. Univ*. Bonn, 1–3.

Ivanov M. 1953: Geologie, Petrographie und Erzlagerstätten des nördlichen teiles des Zips-Gömörer Erzgebirges zwischen Kluknava und Žakarovce. [Geologicko-petrografické a rudné pomery v severnej časti Spišsko-gemerského rudohoria.] *Geol. Zbor. Geol. Carpath.* 4, 705–751 (in Slovak with German and Russian summary).

Kozur H. 1991: The evolution of the Meliata-Hallstatt ocean and its significance for the early evolutiom of the Eastern Alps and Western Carpathians. *Paleogeogr. Paleoclimatol. Palaeoecol*. 87, 109–135.

Krainer K. 1993: Late- and Post-Variscan Sediments of the Eastern and Southern Alps. In: von Raumer J.F. & F. Neubauer (Eds.): Pre-Mesozoic geology in the Alps. *Springer-Verlag*, 537–564.

Ludwig K.R. 1999: User's manual for Isoploths/Ex, Version 2.10, A geochronological toolkit for Microsoft Excel. *Berkeley Geochronology Center*, *Spec. Publ.* No. 1a, 2455 Ridge Road, Berkeley CA 94709, USA.

Ludwig K.R. 2000: SQUID 1.00, A User's Manual. *Berkeley Geochronology Center*, *Spec. Publ.* No. 2, 2455 Ridge Road, Berkeley, CA 94709, USA.

Mazzoli C., Sassi R. & Vozárová A. 1992: The pressure character of the Alpine metamorphism in the Central and Inner Western Carpathians (Czecho-Slovakia). In: Vozár J. (Ed.): Spec. Vol. IGCP No. 276. *D. Štúr Inst. Geol*., Bratislava, 109–117.

Mello J., Elečko M., Pristaš J., Reichwalder P., Snopko L., Vass D., Vozárová A., Gaál L., Hanzel V., Hók J., Kováč P., Slavkay M. & Steiner A. 1997: Explanation to Geological Map of the Slovenský kras Mts. *D. Štúr Publ.,* Bratislava, 1–225 (in Slovak).

Mello J., Reichwalder P. & Vozárová A. 1998: Bôrka Nappe: high-pressure relic from the subduction-accretion prism of the Meliata Ocean (Inner Western Carpathians, Slovakia). *Slovak Geol. Mag*. 4, 261–273.

Naumann E.R., Olsen K.H., Baldridge W.S. & Sundvall B. 1992: The Oslo Rift: A review. *Tectonophysics* 1–3, 1–18.

Pearce J.A., Harris N.B.W. & Tindle A.G. 1984: Trace elements discrimination diagrams for the tectonic interpretation of granitic rocks. *J. Petrology* 25, 956–983.

Rojkovič I. & Konečný P. 2005: Th-U-Pb dating of monazite from the Cretaceous uranium vein mineralization in the Permian rocks of the Western Carpathians. *Geol. Carpathica* 56, 493–502.

Rojkovič I. & Vozár J. 1972: Contribution to the relationship of the Permian volcanism in the northern Gemerides and Choč Unit. *Geol. Zbor. Geol. Carpath.* 23, 87–98.

Stacey J.S. & Kramers J.D. 1975: Approximation of terrestrial lead isotope evolution by a two-stage model. *Earth Planet. Sci. Lett.* 26, 207–221.

Stampfli G.M., Von Raumer J. & Borel G.D. 2002: The Paleozoic evolution of pre-Variscan terranes: From peri-Gondwana to Variscan collision. *Geol. Soc. Amer., Spec. Pap.* 364, 263–280.

Šucha V. & Eberl D.D. 1992: Postsedimentary alteration of the Permian sediments in the northern Gemericum and Hronicum of the Western Carpathians. *Miner. Slovaca* 24, 399–405 (in Slovak).

Taylor S.R. & McLennan S.M. 1985: The continental crust: its composition and evolution. *Blackwell,* Oxford, 1–312.

Václav J. & Vozárová A. 1978: Characteristic of the Northern Gemeric Permian in the Košická Belá area. *Západ. Karpaty, Sér. Mineral. Petrogr. Geochém. Metalogen.* 5, *GÚDŠ*, Bratislava, 83–108 (in Slovak).

Vozárová A. 1996: Tectono-sedimentary evolution of Late Paleozoic basins based on interpretation of lithostratigraphic data (Western Carpathians; Slovakia). *Slovak Geol. Mag.,* 3–4/96, *D. Štúr Publ*., Bratislava, 251–271.

Vozárová A., Šmelko M. & Paderin I. 2009a: Permian single crystal U-Pb zircon age of the Rožňava Formation volcanites (Southern Gemeric Unit, Western Carpathians, Slovakia). *Geol. Carpathica* 60, 6, 439–448. Doi: 10.2478/v10096-009-0032-1

Vozárová A., Ebner F., Kovács S., Kräutner H.-G., Szederkenyi T., Krstić B., Sremac J., Aljinovic D., Novak M. & Skaberne D. 2009b: Late Variscan (Carboniferous to Permian) environments in the Circum Pannonian Region. *Geol. Carpathica* 60, 1, 71–104. Doi: 10.2478/v10096-009-0002-7

Wiedenbeck M., Allé P., Corfu F., Griffin W.L., Meier M., Oberli F., Von Quadt A., Roddick J.C. & Spiegel W. 1995: Three natural zircon standards for U-Th-Pb, Lu-Hf, trace element and REE analyses. *Geostandards Newsletter* 19, 1–23.

Williams I.S. 1998: U-Th-Pb Geochronology by ion microprobe. In: McKibben M.A., Shanks III. W.C. & Ridley W.I. (Eds.): Applications of microanalytical techniques to understanding mineralizing processes. *Rev. Econ. Geol.* 7, 1–35.

Winchester J.A. & Floyd P.A. 1977: Geochemical discrimination of different magma series and differentiation products using immobile elements. *Chem. Geol*. 20, 325–343.

Ziegler A.M. 1990: Phytogeographic patterns and continental configurations during the Permian Period. In: McKerrow W.S. & Scotese C.R. (Eds.): Palaeozoic palaeogeography and biogeography. *Geol. Soc. London, Mem.* 12, 263–379.

Appendix

Selected CL zircon images from the Permian volcanites from the Northern Gemeric Unit (samples 38/SM and 16/SM) and from the Bôrka Nappe (sample 22/SM) and age data based on $^{206}Pb/^{238}U$ ratios with indication of measurement points.